

Preparation of Nd–Fe–B nanoparticles by surfactant-assisted ball milling technique

M. Yue,^{a)} Y. P. Wang, N. Poudyal, C. B. Rong, and J. P. Liu^{b)}

Department of Physics, University of Texas at Arlington, Arlington, Texas 76019, USA

(Presented 11 November 2008; received 17 September 2008; accepted 21 October 2008; published online 12 February 2009)

Nd–Fe–B nanoparticles have been obtained by using surfactant-assisted ball milling and subsequent size-selection technique. Structural analyses show that nanoparticles with two particle sizes around 10 and 100 nm were obtained. The partially amorphous Nd–Fe–B nanoparticles give their room-temperature coercivities around 0.1 and 1.5 kOe for the small and large nanoparticles, respectively. As the temperature decreases to 200 K, the coercive force of the large nanoparticles increases by 50% due to the enhancement of the magnetocrystalline anisotropy of the Nd₂Fe₁₄B phase in the particles. © 2009 American Institute of Physics. [DOI: 10.1063/1.3059228]

I. INTRODUCTION

As a promising candidate in applications in high density magnetic recording and high-performance nanocomposite magnets, permanent magnetic nanoparticles have drawn tremendous attention in recent years.^{1–3} A series of preparation techniques such as chemical synthesis, electrodeposition, and high energy ball milling have been developed to fabricate permanent magnetic nanoparticles with different chemical compositions.^{1–7} In our previous study, SmCo₅ and Sm₂Co₁₇ nanoparticles with different sizes and narrow size distribution were prepared via surfactant-assisted high energy ball milling and subsequent size selection. High coercive force of 3.1 kOe for Sm₂Co₁₇ nanoparticles at room temperature was obtained.⁶ In this study, we apply this technique to prepare Nd–Fe–B nanoparticles with desirable structural and magnetic properties.

II. EXPERIMENTAL

The starting powders used in our study are the MQ-C Nd–Fe–B ribbons from Magnequench Company. Heptane (99.8% purity) was used as the solvent and oleic acid (90%) and oleyl amine (98%) were used as the surfactants during milling. The powders were ground in a milling vial with stainless balls by using a Spex 8000M high energy ball milling machine, and the weight ratio of the powders to the balls is 1:10. The amount of solvent and surfactants used was about 50% and 10% of the weight of the starting powders, respectively. After 12 h milling, the resultant slurry was then dispersed into heptane solvent by ultrasonic vibration and transferred to centrifugal tubes for size selection which was controlled by the time of the settling down process.

Samples for magnetic characterization were prepared by mixing the nanoparticles in epoxy under pure argon atmosphere. A Quantum Design magnetic properties measurement system magnetometer was used in magnetic measurement.

Structural and morphological characterizations were made using x-ray diffraction (XRD) and a transmission electron microscopy (TEM). Size distribution of the nanoparticles was examined by a NanoTrac laser particle size analyzer (LPSA).

III. RESULTS AND DISCUSSIONS

Figures 1(a) and 1(b) show TEM images of the small and big Nd–Fe–B nanoparticles, respectively. To collect the small size nanoparticles, the as-milled Nd–Fe–B slurry was ultrasonically vibrated with heptane solvent and settled down for 20 h, during which large particles sedimented gradually while smaller particles were still floating in the solution. To obtain the larger nanoparticles, the slurry was washed once in heptane to remove the smallest floating nanoparticles. Then the remaining part was transferred into a surfactant-coated centrifugal tube and dispersed in heptane again by similar ultrasonic vibration process; the dispersed solution was then settled down for 3 h. After this settling-down time, a low-speed centrifugal separation of 500 rpm was done to remove the largest particles. It can be seen from Fig. 1 that both the small and large nanoparticles exhibit irregular shape. It was observed that there is severe agglomeration in

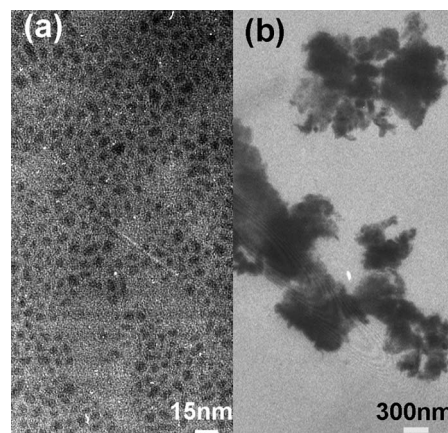


FIG. 1. TEM images of (a) small and (b) big Nd–Fe–B nanoparticles.

^{a)}Electronic mail: yueming@bjut.edu.cn.

^{b)}Author to whom correspondence should be addressed. Electronic mail: pliu@uta.edu.

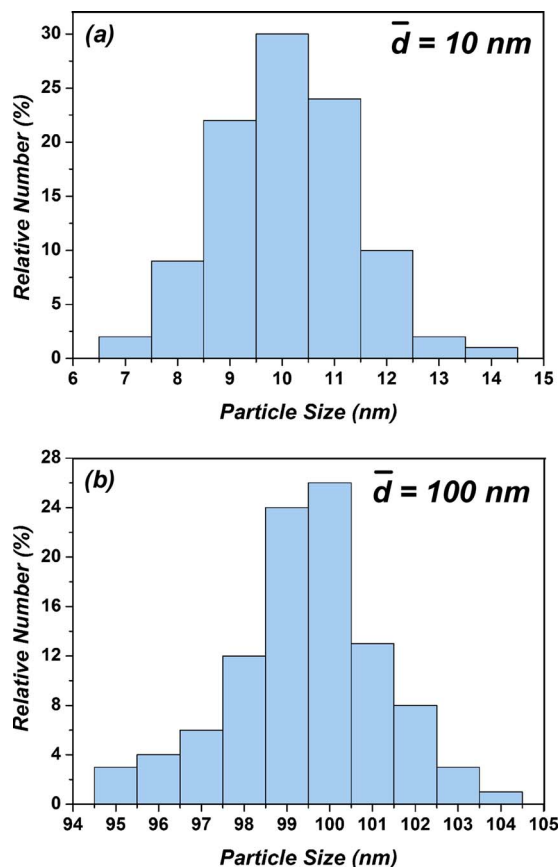


FIG. 2. (Color online) The size distribution of the (a) small and (b) big Nd-Fe-B nanoparticles.

the large nanoparticles, as seen from the TEM image of the large nanoparticles. This may be attributed to the strong magnetic attraction between the ferromagnetic nanoparticles. To further determine the particle size, LPSA was applied to measure the particle size. It shows that the average size of the small and big particles are 10 and 100 nm, respectively, and both samples of the nanoparticles possess narrow size distribution, which was shown in Figs 2(a) and 2(b), respectively.

Figure 3 shows the XRD patterns of the Nd-Fe-B nanoparticles with different sizes obtained by the size selection process. For comparison, the pattern of the starting ribbons was also shown in Fig. 3. It is found that both diffraction peaks of the small and the large nanoparticles broadened into big humps. Apart from the decrease in the particle size, the strains and amorphization induced during ball milling process may also contribute to the broadening of the diffraction peaks. It is therefore difficult to quantitatively calculate the particle size from the width of the diffraction peaks. In addition, no diffraction peaks from rare earth oxides were found in both patterns for the small and the large nanoparticles, while those peaks always showed up in the XRD patterns of oxidized Nd-Fe-B nanoparticles in our other experiments when the atmosphere was not well controlled. This observation indicates that the prepared nanoparticles have effectively protected from oxidation during the fabrication and examination processes.

Figure 4 shows the magnetization hysteresis loop of both

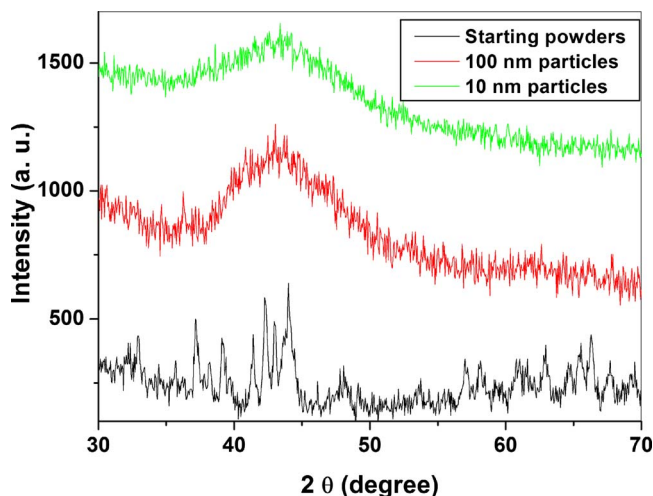


FIG. 3. (Color online) XRD patterns of small and big Nd-Fe-B nanoparticles, and the starting Nd-Fe-B ribbons.

the small and the large Nd-Fe-B nanoparticles at 300 K. It should be mentioned that the quantitative determination of the magnetization of the particles is difficult due to the effect of epoxy and surfactants that cover the particles. The intrinsic coercive forces of the small and big nanoparticles are 0.1 and 1.5 kOe, respectively, which is far lower than 17 kOe of coercive force of the starting ribbons. The significant reduction in the coercive force may be due to the amorphous structure of the nanoparticles and some possible contamination during the preparation process. Furthermore, it is also found that the coercive force of the large nanoparticles increases by 50% as the measuring temperature down to 200 K due to the enhancement of the magnetocrystalline anisotropy of the $\text{Nd}_2\text{Fe}_{14}\text{B}$ phase in the particles. However, similar increase was not detected in the small nanoparticles, indicating that the small particles are more prone to amorphization and oxidation, which may result in more structural change in the $\text{Nd}_2\text{Fe}_{14}\text{B}$ phase during preparation process, compared with the large particles.

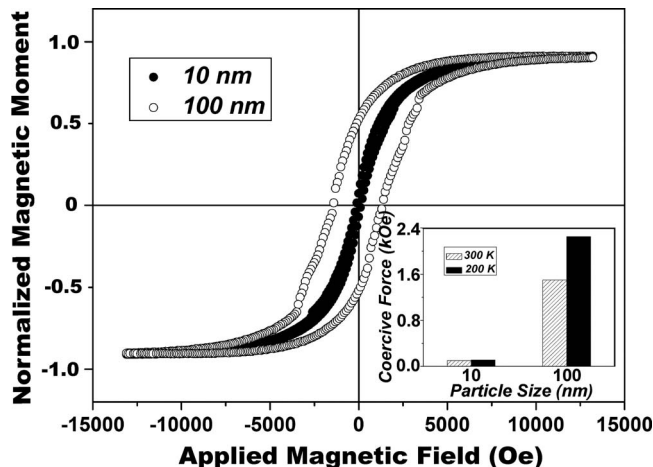


FIG. 4. The magnetization hysteresis loop of both the small and big Nd-Fe-B nanoparticles at 300 K. Inset: intrinsic coercive force of the particles vs measuring temperature.

IV. CONCLUDING REMARKS

In summary, Nd–Fe–B nanoparticles with different sizes were prepared by surfactant-assisted ball milling technique. By subsequent size selection, nanoparticles with average particle size of 10 and 100 nm were obtained. XRD patterns of both the small and the large particles broaden into a big hump, indicating partially amorphous state of the particles induced by the high energy during ball milling process. Magnetic measurements show that the room-temperature coercive forces of the small and the large nanoparticles are 0.1 and 1.5 kOe, respectively. The coercive force of the large nanoparticles increases by 50% as the temperature drops to 200 K due to the enhancement of the magnetocrystalline anisotropy of the Nd₂Fe₁₄B phase in the particles.

ACKNOWLEDGMENTS

This work is supported by U.S. DoD/DARPA. The authors thank Dr. Zhongmin Chen of Magnequench Co. for providing the Nd–Fe–B ribbons.

- ¹S. Sun, C. B. Murray, D. Weller, L. Folks, and A. Moser, *Science* **287**, 1989 (2000).
- ²H. Zeng, J. Li, J. P. Liu, Z. L. Wang, and S. Sun, *Nature (London)* **420**, 395 (2002).
- ³C. B. Rong, V. Nandwana, N. Poudyal, J. Ping Liu, M. E. Kozlov, R. H. Baughman, Y. Ding, and Z. L. Wang, *J. Appl. Phys.* **102**, 023908 (2007).
- ⁴V. M. Chakka, B. Altuncevhahir, Z. Q. Jin, Y. Li, and J. P. Liu, *J. Appl. Phys.* **99**, 08E912 (2006).
- ⁵J. Zhang, P. Evans, and G. Zangari, *J. Magn. Magn. Mater.* **283**, 89 (2004).
- ⁶S. Stoyanov, V. Skumryev, Y. Zhang, Y. Huang, G. Hadjipanayis, and J. Nogues, *J. Appl. Phys.* **93**, 7592 (2003).
- ⁷Y. P. Wang, Y. Li, C. B. Rong, and J. P. Liu, *Nanotechnology* **18**, 465701 (2007).